
Bayesian Neural Ordinary Differential Equations

Raj Dandekar

Massachusetts Institute of Technology
rajd@mit.edu

Vaibhav Dixit

Julia Computing Inc.

Mohamed Tarek

University of New South Wales at Canberra, Australia

Aslan García-Valadez

National Autonomous University of Mexico.

Chris Rackauckas

Massachusetts Institute of Technology,
University of Maryland Baltimore
crackauc@mit.edu

Abstract

Recently, Neural Ordinary Differential Equations has emerged as a powerful framework for modeling physical simulations without explicitly defining the ODEs governing the system, but learning them via machine learning. However, the question: “Can Bayesian learning frameworks be integrated with Neural ODE’s to robustly quantify the uncertainty in the weights of a Neural ODE?” remains unanswered. In an effort to address this question, we demonstrate the successful integration of Neural ODEs with two methods of Bayesian Inference: (a) The No-U-Turn MCMC sampler (NUTS) and (b) Stochastic Langevin Gradient Descent (SGLD). We test the performance of our Bayesian Neural ODE approach on classical physical systems, as well as on standard machine learning datasets like MNIST, using GPU acceleration. Finally, considering a simple example, we demonstrate the probabilistic identification of model specification in partially-described dynamical systems using universal ordinary differential equations. Together, this gives a scientific machine learning tool for probabilistic estimation of epistemic uncertainties.

1 Introduction

The underlying scientific laws describing the physical world around us are often prescribed in terms of ordinary differential equations (ODEs). Recently, Neural Ordinary Differential Equations [4] has emerged as a powerful framework for modeling physical simulations without explicitly defining the ODEs governing the system, but learning them via machine learning. By noticing that in the limit of infinite layers, a ResNet module [7] behaves as a continuous time ODE, Neural ODEs allow the coupling of neural networks as expressive function transformations, and powerful purpose built ODE solvers. While [4] explored a number of applications of the Neural ODE framework, their success in a Bayesian inference framework remains unexplored.

Simultaneously, there has been an emergence of efficient Bayesian inference methods suited for high-dimensional parameter systems, such as the No-U-Turn MCMC sampler (NUTS) [11] which

is an extension of the Hamiltonian Monte Carlo Algorithm, and Stochastic Gradient Markov Chain Monte Carlo (SGMCMC) methods like Stochastic Gradient Langevin Descent (SGLD) [29].

A number of works in literature explored the use of Bayesian methods to infer parameters of systems defined by ODEs [19, 26, 6, 12] and others used Bayesian methods to infer parameters of neural network models, e.g. [15, 20, 13]. Bayesian neural networks in particular has been an active area of research for a while. The readers are referred to the excellent recent tutorial by [15] for an overview of recent advances in the field. However, this prompts the question: “Can Bayesian learning frameworks be integrated with Neural ODE’s to robustly quantify the uncertainty in the weights of a Neural ODE?”

In an effort to address this question, we demonstrate and compare the integration of Neural ODEs with two methods of Bayesian Inference: (a) The No-U-Turn MCMC sampler (NUTS) [11] and (b) Stochastic Langevin Gradient Descent (SGLD) [29]. For the SGLD sampler, through GPU acceleration, we are able to get Bayesian estimates of the test prediction accuracy for the standard MNIST dataset; which has not been done previously using Neural ODEs.

Finally, instead of learning the entire differential equation governing a physical system as done by Neural ODEs, we consider the problem of recovering missing terms from a dynamical system using universal differential equations (UDEs) [22]. Using a variation of the SGLD called Preconditioned SGLD, we demonstrate the Bayesian version of UDEs on a simple test case which is accurately able to symbolically identify model specifications. Together this demonstrates a viable method for probabilistic quantification of epistemic uncertainties via a hybrid machine learning and mechanistic model-based technique.

Our approach differs from that of [1] who mainly looked at integration of Bayesian methods with Neural SDE’s, and not Neural ODEs describing physical systems or large scale deep learning datasets like the MNIST dataset, which we consider here.

In this study, we used the Julia differentiable programming stack [21] to compose the Julia differential equation solvers [23] with the Turing probabilistic programming language [5, 30]. The study was performed without modifications to the underlying libraries due to the composability afforded by the differentiable programming stack.

2 Results

We illustrate the robustness of the Bayesian Neural ODE framework by performing tests on the following cases:

Case study 1: Spiral ODE

The Spiral ODE is prescribed by the following system of equations

$$\frac{du_1}{dt} = -\alpha u_1^3 + \beta u_2^3 \quad (1)$$

$$\frac{du_2}{dt} = -\beta u_1^3 - \alpha u_2^3 \quad (2)$$

Case study 2: Lotka Volterra ODE

The Lotka Volterra system of equations is prescribed by the following system of ODEs

$$\frac{du_1}{dt} = -\alpha u_1 - \beta u_1 u_2 \quad (3)$$

$$\frac{du_2}{dt} = -\delta u_2 + \gamma u_1 u_2 \quad (4)$$

2.1 Bayesian Neural ODE: NUTS Sampler

The No-U-Turn-Sampler (NUTS) is an extension of the Hamiltonian Monte Carlo (HMC) algorithm. Through a recursive algorithm, NUTS automatically determines when the sampler should stop an

iteration, and thus prevents the need to specify user defined parameters, like the number of steps L . In addition, through a dual averaging algorithm, NUTS adapts the step size ϵ throughout the sampling process.

We define the parameters of the d dimensional Neural ODE by θ . The action of the Neural ODE on an input value u_0 generates an output $\tilde{Y} = \text{NNODE}_\theta(u_0)$. The input data is denoted by \hat{Y} . The loss function, L is defined as

$$L(\theta) = \sum_{i=1}^d \|\hat{Y}_i - \tilde{Y}_i\|^2 \quad (5)$$

The model variables θ and the momentum variables r are drawn from the joint distribution

$$p(\theta, r) \propto \exp[\mathcal{L}(\theta) - \frac{1}{2}r \cdot r] \quad (6)$$

where \mathcal{L} is the logarithm of the joint density of θ . In terms of a physical analogy, if θ denotes a particle's position, then \mathcal{L} can also be viewed as the negative of the potential energy function and $\frac{1}{2}r \cdot r$ denotes the kinetic energy of the particle.

In the Bayesian Neural ODE framework, we define $\mathcal{L}(\theta)$ as

$$\mathcal{L}(\theta) = - \sum_{i=1}^d \|\hat{Y}_i - \tilde{Y}_i\|^2 - \theta \cdot \theta \quad (7)$$

The $\theta \cdot \theta$ term indicates the use of Gaussian priors. We adapt the step size of the leapfrog integrator using Nesterov's dual averaging algorithm [11] with δ as the target acceptance rate. Finally, we define the number of warmup samples as n_w and the number of posterior samples collected as n_p .

We apply the Bayesian Neural ODE framework outlined above to case studies 1 and 2 given in Equations 1-4. For case study 1, we use $\alpha = 0.1, \beta = 2$. In the NUTS algorithm, we use $\delta = 0.45, n_w = 1000, n_s = 500$. For case study 2, we use $\alpha = 1.5, \beta = 1, \gamma = 3, \delta = 1$; with $\delta = 0.45, n_w = 500, n_s = 1000$. 2 layers with 50 units in each layer and tanh activation function was used as the neural ODE architecture for both examples.

From figure 1, we can see that the Bayesian Neural ODE: NUTS prediction and forecasting for both case studies outlined in Equations 1-4 are consistent with the ground truth data.

Figure 2a showing the posterior density and trace plots for the first 5 parameters of the Spiral ODE example, shows that the samples are well mixed. The quick decay seen in the auto-correlation plot shown in figure 2b also indicates a fast mixing Markov chain. This is also confirmed by the effective sample size extracted for the posterior chain of 500 samples, which shows values of 362, 470, 134, 509, 661 for the first 5 parameters. Similar well mixed plots are seen for all parameters, but are not shown here for the sake of brevity.

Table 1 shows the effect of NUTS acceptance ratio and Neural ODE architecture on the Bayesian Neural ODE performance for the Spiral ODE example. The minimum loss value obtain is similar in all cases shown. Thus, we see that even the smallest neural architecture with 2 layers and 5 units in each layer gives the optimal loss performance, and with a considerably better timing performance. Among different NUTS acceptance ratios (δ) tested, the best timing performance is given by the lowest acceptance ratio, $\delta = 0.45$.

2.2 Bayesian Neural ODE: SGLD

Stochastic Gradient Langevin Dynamics (SGLD) is an adaptation, designed to sample from the posterior as the iterations increase, of the usual stochastic gradient descent algorithm. In each

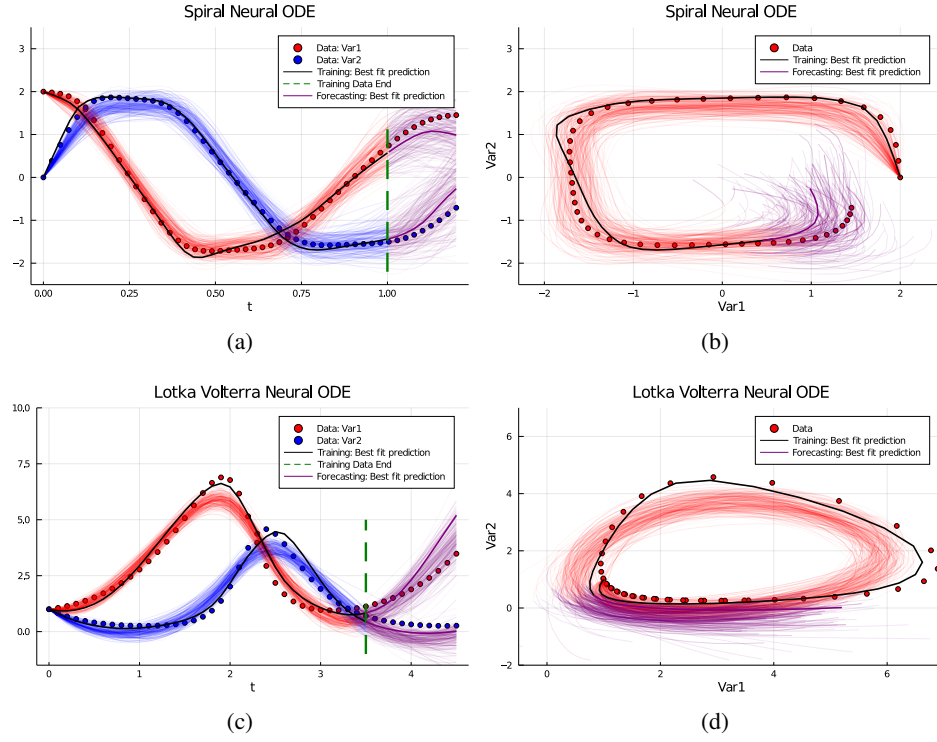


Figure 1: Comparison of the Bayesian Neural ODE: NUTS prediction and estimation compared with data for (a,b) Case study 1 and (c,d) Case study 2.

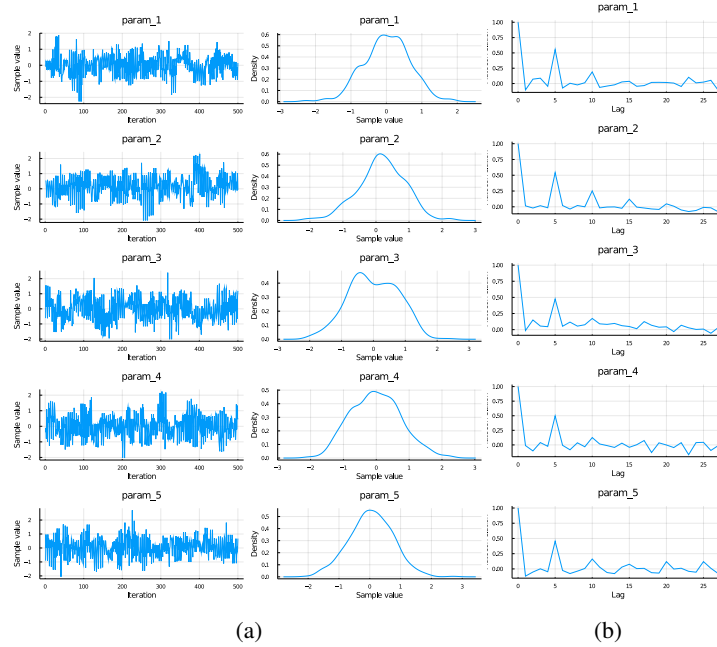


Figure 2: For the Spiral ODE example (Equations 1-2), using the NUTS framework, figure shows: (a) Trace plots and Density plots of the posterior and (b) auto-correlation plot for the first 5 parameters.

Table 1: Spiral ODE: Effect of NUTS acceptance ratio and Neural ODE architecture. Number of warmup samples, $n_w = 500$ and number of posterior samples, $n_s = 500$ for all cases shown. The minimum loss value obtain is similar in all cases shown.

δ	Units	Layers	Time (s)
0.45	5	2	480
0.45	10	2	900
0.45	50	2	2100
0.45	100	2	3900
0.45	10	3	3300
0.45	10	4	10200
0.65	50	2	3400
0.85	50	2	7900
0.95	50	2	8600

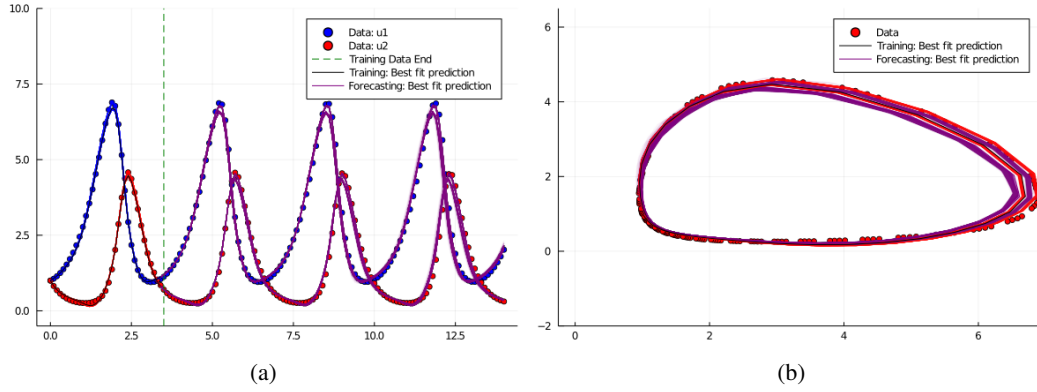


Figure 3: Comparison of the Bayesian Neural ODE: SGLD estimation and data for the Lotka Volterra ODE case study shown as (a) time series plots and (b) contour plots.

iteration, we update our vector θ of parameters according to the rule

$$\theta_t := \theta_t - \Delta\theta_t \quad (8)$$

$$\Delta\theta_t := \frac{\epsilon_t}{2} \left(\nabla \log p(\theta_t) + \frac{1}{n} \sum_{i=1}^n \nabla \log p(\mathcal{D}_n | \theta) \right) + \eta_t \quad (9)$$

$$\eta_t \sim \mathcal{N}(0, \epsilon_t) \quad (10)$$

where \mathcal{D}_n are the minibatches the training dataset \mathcal{D} has been split into. $p(\mathcal{D}_n | \theta)$ is the likelihood, whose logarithm is equivalent to the loss function, and $p(\theta_t)$ is any priors, also known as regularisation terms, imposed onto the parameters θ . The stepsizes ϵ_t must follow a decaying scheme which satisfies the conditions [29]:

$$\sum_{t=1}^{\infty} \epsilon_t = \infty \quad \sum_{t=1}^{\infty} \epsilon_t^2 < \infty \quad (11)$$

in this article we have chose a polynomial decaying scheme $\epsilon_t = a(b + t)^{-\gamma}$ with a, b , and γ as tuneable hyperparameters.

The update scheme for θ is composed of two stages. In the first stage, where the approximate gradient dominates, we approach the regions with higher mass probability. During the second phase, instead of allowing θ to converge to a single value, it walks randomly with a predominantly Gaussian noise since the gradient is $\mathcal{O}(\epsilon_t)$ and the Gaussian noise is $\mathcal{O}(\sqrt{\epsilon_t})$. It is on this second stage where it is theoretically guaranteed to converge to the posterior, and hence, we may use this stage to sample parameters from the posterior.

We now apply SGLD on the Lotka Volterra system in Equations 3-4. The Lotka Volterra system used in this case has the same parameters as the one used for NUTS. Again, we apply SGLD with

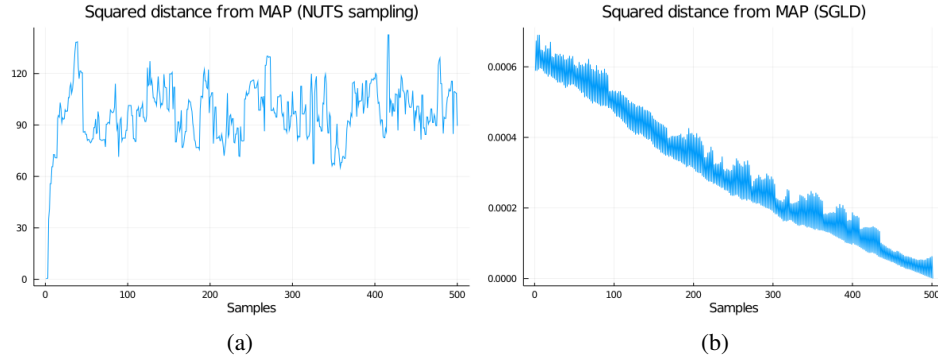


Figure 4: (a) Figure shows that for the NUTS sample initialized at the MAP point, the sampler quickly jumps away from the MAP point and never returns back. (b) Figure shows that for the SGLD sampler initialized at the MAP, all posteriors samplers are close to the MAP point.

Table 2: Performance on MNIST using the Bayesian Neural ODE: SGLD approach outlined in the present study. Out of the 310 posterior samples for each image in a batch of 128 images considered, the best fit test error represents if at least one sample out of the 310 gave the correct answer. The mean test error takes the mean of the number of erroneous predictions in all samples for all images.

	Error estimates?	Neural ODE?	Best fit test error	Mean test error	Reference
RK-Net	✗	✓	0.47 %	-	Chen et al. (2018)
ODE-Net	✗	✓	0.42 %	-	Chen et al. (2018)
Bayesian Alex-Net	✓	✗	1 %	-	Shridhar et al. (2019)
Bayesian LeNet-5	✓	✗	2 %	-	Shridhar et al. (2019)
Bayesian Neural ODE	✓	✓	2.30 %	15.42%	Our study

45000 iterations and sampled the last 2000 updates. The hyperparameters used were $a = 0.0025$, $b = 0.05$, $\gamma = 0.35$. The neural ODE architecture was again 2 layers with 50 neurons and tanh activation. The algorithm took approximately 679 seconds to run.

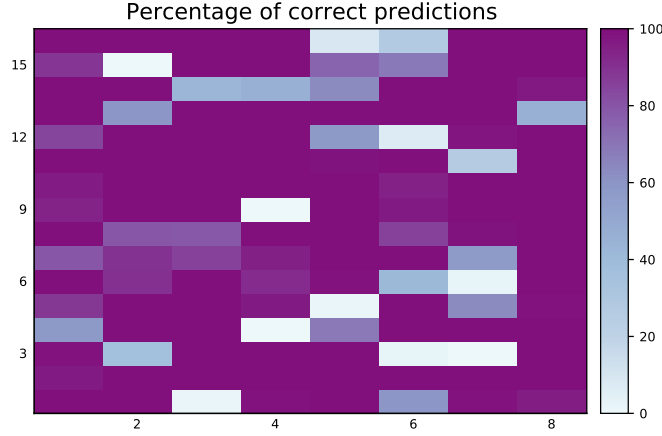
From figure 3 we notice a good fit on the training dataset. The Bayesian Neural ODE trained using the SGLD approach has accurately captured the periodicity of the system; and is seen to generalize for a much longer duration than the NUTS sampler.

2.2.1 Comparison between SGLD and NUTS

Through figures 1 and 3, we note that SGLD generally has a better mean prediction accuracy than NUTS. This can be attributed to the non-convexity/multi-modality of the likelihood function where the MAP point is likely to be in a region with low probability mass, leading the NUTS sampler which uses non-stochastic gradients to not "find" the region surrounding the MAP point in the time of the sampling. The use of stochastic gradients in SGLD seems to have led to a sample much closer to the MAP point and with a much lower mean prediction error. This difference between NUTS and SGLD is illustrated in figure 4, where the distance of the posterior samples from the MAP point is shown. Figure 4a shows that for the NUTS sample initialized at the MAP point, the sampler quickly jumps away from the MAP point and never returns back. Figure 4b shows that for the SGLD sampler, all posteriors samplers are much closer to the MAP point, than the NUTS sampler.

2.2.2 SGLD on the MNIST dataset

We focus now on a classification task on the MNIST benchmark dataset. As mentioned in the introduction, a Neural ODE layer can be interpreted as a continuous residual layer. Residual layers are often used in image recognition, so it is natural to implement ODE layers instead of residual layers in an image recognition architecture. We use three convolutional layers with a 3×3 filter, 1×1 padding and ReLU activations, interspersed with a max-pooling layer of 2×2 . Then, we put



(a)

Figure 5: Bayesian Neural ODE: SGLD method is applied to the MNIST dataset. Each cell in this figure represents the percentage of correct predictions out of 311 posterior samples on a single image. Results for a batch of 128 images have been shown in the form of a heatmap

two Neural ODE layers (acting as two residual layers) and finally a fully connected layer with 10 neurons (one per class).

We use SGLD with parameters $a = 0.05$, $b = 0.5$, $\gamma = 0.5$ and run for 2110 iterations and sampled the last 310 parameter updates. It is observed that using SGLD is more expensive computationally, requiring five epochs through the training dataset, than a simple MAP estimation. A trial MAP optimisation using ADAM was run with a single epoch resulting in a 97.8% test accuracy.

Each cell in figure 5 represents the percentage of correct predictions out of 310 posterior samples on a single image. Results for a batch of 128 images have been shown in the form of a heatmap. Table 2 shows the performance of this Bayesian approach on the MNIST data. Out of the 310 posterior samples for each image in a batch of 128 images considered, the best fit test error represents if at least one sample out of the 310 gave the correct answer. The mean test error takes the mean of the number of erroneous predictions in all samples for all images.

From table 2, we note that previous architectures for MNIST analysis either have a Neural ODE architecture without error estimates [4] or do not incorporate a Neural ODE for error estimation [25]. In our approach, we not only incorporate a Neural ODE into our architecture, but also encode the confidence of our prediction. Although there is a lot of further scope of improving the test accuracy, this is the first time a Bayesian Neural ODE approach has been combined with a large ML dataset. Future studies would be focused on comparison of our method with studies pertaining to Bayesian Neural Networks integrated with Stochastic Differential Equations [1] and Variational Inference [31].

2.3 Bayesian Neural ODE: Variational Inference

It should be noted that we also tried the family of Bayesian methods generally used in combination with solving deep learning problems: Variational Inference [9, 28, 14, 10, 24, 16, 8]. Using the ADVI (Automatic Differentiation Variational Inference) framework [17] with samples per step = 10 and the maximum number of gradient steps = 1000.

Figure 6a, b shows the poor estimation and generalization performance of the Bayesian Neural ODE: Variational Inference framework applied to the Lotka Volterra dataset, compared to NUTS (figure 1b). Due to the poor performance of Variational Inference observed, this framework was not further explored in this study. Future work would focus on integration of Variational Inference with Normalizing Flows; thus using neural networks as transformation functions to approximate the target distribution better.

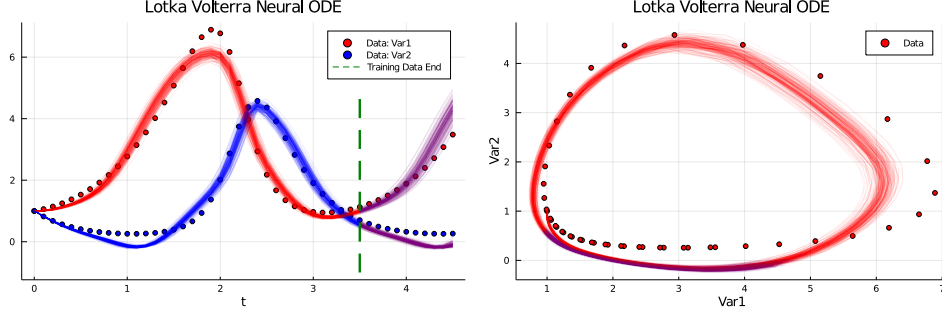


Figure 6: Comparison of the Bayesian Neural ODE: Variational Inference prediction and estimation compared with data for the Lotka Volterra Case study 2.

2.4 Bayesian Neural UDE

2.4.1 Preconditioned SGLD (PSGLD)

More efficient training of deep neural networks is achieved by using a preconditioned matrix $G(\theta)$ in the gradient update step of Equation 9 [18]. Combining this with an adaptive step size method like RMSprop leads to much faster sampling than the standard SGLD approach, as outlined in the Preconditioned SGLD with RMSprop algorithm by [18]. We demonstrate the use of this algorithm in this section, where standard SGLD failed to converge to the true posterior.

As outlined by [22], universal differential equations (UDE's) can be used to recover missing terms of governing equations describing dynamical systems. As an example, we look at the Lotka Volterra system with a missing term denoted by $M(u_1, u_2)$ in the first variable derivative as

$$\frac{du_1}{dt} = -\alpha u_1 - M(u_1, u_2) \quad (12)$$

$$\frac{du_2}{dt} = -\delta u_2 + \gamma u_1 u_2 \quad (13)$$

$$(14)$$

Using the PSGLD method described in (2.4.1), as outlined in [22], we trained $M_\theta(u_1, u_2)$ as a neural network to optimize the weights θ ; and recover the missing term time series. We sampled from the last 100 updates of the converged sampler. Figure 7a shows that the recovered time series $M_\theta(u_1, u_2)$ from 100 trajectories matches very well with the actual term $M_\theta(u_1, u_2) = u_1 u_2$. These optimized parameter space for all 100 trajectories lies very close to each other, indicating that the PSGLD method indeed converges and then subsequently samples closer to the true posterior.

Subsequently, we used a sparse regression technique called Sequential Thresholded Ridge Regression (STRRidge) algorithm [3] on the neural network output to reconstruct the missing dynamical equations for 100 trajectories of the sampled parameter space. The STRRidge algorithm has a tunable sparsity parameter λ to control the sparsity of the obtained dominant terms. Optimally, we would want the sparsest solution with the least possible error.

Figure 7b shows the variation of the number of terms recovered by the STRRidge algorithm with the sparsity parameter, λ ; which shows a decreasing trend as expected. The colorbar indicates the error between the sparse recovered solution and the neural network output $M_\theta(u_1, u_2)$. It can be seen that the highlighted box indicates the optimal point which has the sparsest solution (1 term) with a very low error. This point also corresponds to the lowest positive AIC score (Akaike Information Criteria) [2, 27] which strives to minimize the model error as well as its complexity (shown in Table 3). Along with showing the AIC score as function of the sparsity parameter λ , table 3 also shows the dominant terms as the sparsity parameter λ is varied.

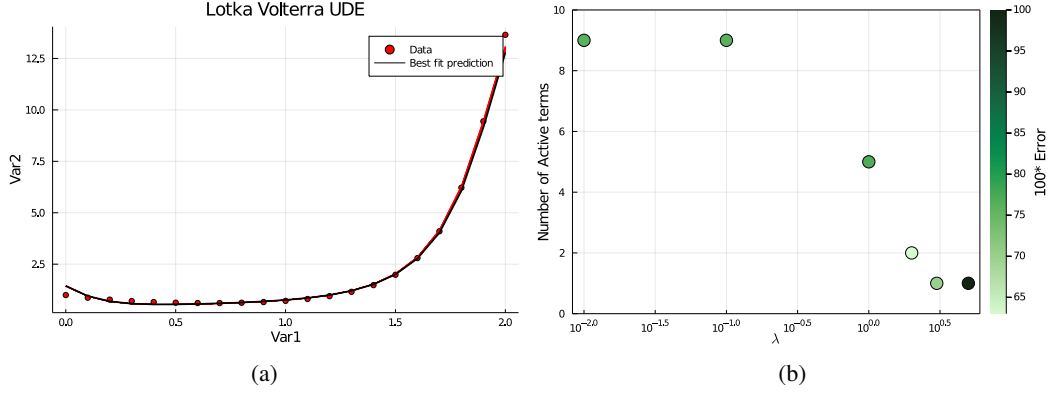


Figure 7: Bayesian Neural UDE estimation is demonstrated for the Lotka Volterra example with a missing term as shown in (12); using the PSGLD approach. (a) Comparison of the recovered missing term and the actual term and (b) Sparsity plot using the STRRidge algorithm. The highlighted box shows the optimal point which gives the sparsest solution (1 term) with a low error. This plot is seen to be the same for 100 trajectories considered in the sampling phase.

Table 3: Bayesian Neural UDE: Recovery of dominant terms for the Lotka Volterra example, as the sparsity parameter λ is varied. Highlighted row shows the sparsity parameter with the lowest positive AIC score.

λ	Number of Active terms	Dominant terms	Error	Mean AIC score	% sampled
0.01	9	$u_1^2, u_2^2, u_1 u_2$ $u_1^2 u_2^2, u_1^2 u_2, u_2^2 u_1$ $u_1 u_2, \text{const}$	0.765	40.4	100
0.1	9	$u_1^2, u_2^2, u_1 u_2$ $u_1^2 u_2^2, u_1^2 u_2, u_2^2 u_1$ $u_1 u_2, \text{const}$	0.764	35	100
1	5	u_1^2, u_2^2, u_2 $u_1^2 u_2, u_1 u_2$	0.764	21.6	100
2	2	$u_1^2 u_2, u_1 u_2$	0.634	7.2	100
3	1	$u_1 u_2$	0.7	4.1	100
5	1	$u_1^2 u_2$	2.49	-1	100

This optimal solution has the quadratic form $\sim u_1 u_2$, for all 100 trajectories indicating that Bayesian Neural UDE approach recovers the correct solution for all sampled trajectories. Out of the 100 models sampled for the optimal sparsity parameter, the model with the lowest AIC score was found to be $M(u_1, u_2) = 0.96 u_1 u_2$, which is very close to the true solution $M(u_1, u_2) = u_1 u_2$. Additionally for all sampled neural networks we see the sample functional forms as the result of the sparsification, indicating that the model discovery is robust to uncertainty. Future work will further identify the relationship between model uncertainties and probabilistic automated discovery.

3 Conclusion and Future work

We have shown that Bayesian learning frameworks can be integrated with Neural ODE's to quantify the uncertainty in the weights of a Neural ODE, using two sampling methods: NUTS and SGLD. Bayesian Neural ODEs with SGLD sampling is seen to provide better prediction accuracy and less bias from the MAP than NUTS sampling, possibly due to non-convexity/multi-modality of the likelihood function where the MAP point is likely to be in a region with low probability mass. However, a better understanding of why the two algorithms differ and how they compare to other algorithms is needed. Further, we show that our Bayesian Neural ODE method can also be used for

standard machine learning datasets like MNIST. Compared to previous architectures for MNIST analysis who either have a Neural ODE architecture without error estimates [4] or do not incorporate a Neural ODE for error estimation [25], we not only incorporate a Neural ODE into our architecture, but also encode the confidence of our prediction. Still, there is a lot of further scope of improving the test accuracy through the use of more complicated architectures, which would be a potential area of future research.

Finally, considering the problem of recovering missing terms from a dynamical system using universal differential equations (UDEs); we demonstrate the Bayesian recovery of missing terms from dynamical systems using a simple example showing the feasibility of the approach.

Currently, it is observed that Bayesian learning of Neural ODEs using NUTS and SGLD is difficult and computationally expensive making it difficult to apply to larger datasets. Therefore, more work is needed to evaluate, understand and improve the convergence of various approximate Bayesian inference and MCMC algorithms in the context of Neural ODEs. In addition to this, follow up work needs to be done to apply the Bayesian Neural UDEs framework to more complicated systems such as epidemiological systems where Neural UDEs can help discover hidden model structure from infection and other population data.

4 Code Availability

All codes are publicly available at https://github.com/RajDandekar/MSML21_BayesianNODE.

References

- [1] Look Andreas and Melih Kandemir. Differential bayesian neural nets. *arXiv preprint arXiv:1912.00796*, 2019.
- [2] Hamparsum Bozdogan. Model selection and akaike’s information criterion (aic): The general theory and its analytical extensions. *Psychometrika*, 52(3):345–370, 1987.
- [3] Steven L Brunton, Joshua L Proctor, and J Nathan Kutz. Discovering governing equations from data by sparse identification of nonlinear dynamical systems. *Proceedings of the national academy of sciences*, 113(15):3932–3937, 2016.
- [4] Ricky TQ Chen, Yulia Rubanova, Jesse Bettencourt, and David K Duvenaud. Neural ordinary differential equations. In *Advances in neural information processing systems*, pages 6571–6583, 2018.
- [5] Hong Ge, Kai Xu, and Zoubin Ghahramani. Turing: a language for flexible probabilistic inference. In *International Conference on Artificial Intelligence and Statistics, AISTATS 2018, 9-11 April 2018, Playa Blanca, Lanzarote, Canary Islands, Spain*, pages 1682–1690, 2018.
- [6] Mark Girolami. Bayesian inference for differential equations. *Theoretical Computer Science*, 408(1):4 – 16, 2008. Computational Methods in Systems Biology.
- [7] Kaiming He, Xiangyu Zhang, Shaoqing Ren, and Jian Sun. Deep residual learning for image recognition. In *Proceedings of the IEEE conference on computer vision and pattern recognition*, pages 770–778, 2016.
- [8] Geoffrey E Hinton, Simon Osindero, and Yee-Whye Teh. A fast learning algorithm for deep belief nets. *Neural computation*, 18(7):1527–1554, 2006.
- [9] Geoffrey E Hinton and Drew Van Camp. Keeping the neural networks simple by minimizing the description length of the weights. In *Proceedings of the sixth annual conference on Computational learning theory*, pages 5–13, 1993.
- [10] Matthew D Hoffman, David M Blei, Chong Wang, and John Paisley. Stochastic variational inference. *The Journal of Machine Learning Research*, 14(1):1303–1347, 2013.
- [11] Matthew D Hoffman and Andrew Gelman. The no-u-turn sampler: adaptively setting path lengths in hamiltonian monte carlo. *J. Mach. Learn. Res.*, 15(1):1593–1623, 2014.
- [12] Hanwen Huang, Andreas Handel, and Xiao Song. A bayesian approach to estimate parameters of ordinary differential equation. *Computational Statistics*, 35(3):1481–1499, Sep 2020.

- [13] Pavel Izmailov, Wesley J. Maddox, Polina Kirichenko, Timur Garipov, Dmitry P. Vetrov, and Andrew Gordon Wilson. Subspace inference for bayesian deep learning. *CoRR*, abs/1907.07504, 2019.
- [14] Michael I Jordan, Zoubin Ghahramani, Tommi S Jaakkola, and Lawrence K Saul. An introduction to variational methods for graphical models. *Machine learning*, 37(2):183–233, 1999.
- [15] Laurent Valentin Jospin, Wray L. Buntine, F. Boussaid, Hamid Laga, and M. Bennamoun. Hands-on bayesian neural networks - a tutorial for deep learning users. *ArXiv*, abs/2007.06823, 2020.
- [16] Diederik P Kingma and Max Welling. Auto-encoding variational bayes. *arXiv preprint arXiv:1312.6114*, 2013.
- [17] Alp Kucukelbir, Dustin Tran, Rajesh Ranganath, Andrew Gelman, and David M Blei. Automatic differentiation variational inference. *The Journal of Machine Learning Research*, 18(1):430–474, 2017.
- [18] Chunyuan Li, Changyou Chen, David Carlson, and Lawrence Carin. Preconditioned stochastic gradient langevin dynamics for deep neural networks. *arXiv preprint arXiv:1512.07666*, 2015.
- [19] David J. Lunn, Nicky Best, Andrew Thomas, Jon Wakefield, and David Spiegelhalter. Bayesian analysis of population pk/pd models: General concepts and software. *Journal of Pharmacokinetics and Pharmacodynamics*, 29(3):271–307, Jun 2002.
- [20] Wesley Maddox, Timur Garipov, Pavel Izmailov, Dmitry P. Vetrov, and Andrew Gordon Wilson. A simple baseline for bayesian uncertainty in deep learning. *CoRR*, abs/1902.02476, 2019.
- [21] Christopher Rackauckas, Alan Edelman, Keno Fischer, Mike Innes, Elliot Saba, Viral B Shah, and Will Tebbutt. Generalized physics-informed learning through language-wide differentiable programming. In *AAAI Spring Symposium: MLPS*, 2020.
- [22] Christopher Rackauckas, Yingbo Ma, Julius Martensen, Collin Warner, Kirill Zubov, Rohit Supekar, Dominic Skinner, and Ali Ramadhan. Universal differential equations for scientific machine learning. *arXiv preprint arXiv:2001.04385*, 2020.
- [23] Christopher Rackauckas and Qing Nie. Differentialequations.jl—a performant and feature-rich ecosystem for solving differential equations in julia. *Journal of Open Research Software*, 5(1), 2017.
- [24] Rajesh Ranganath, Sean Gerrish, and David Blei. Black box variational inference. In *Artificial Intelligence and Statistics*, pages 814–822. PMLR, 2014.
- [25] Kumar Shridhar, Felix Laumann, and Marcus Liwicki. A comprehensive guide to bayesian convolutional neural network with variational inference. *arXiv preprint arXiv:1901.02731*, 2019.
- [26] Udo von Toussaint. Bayesian inference in physics. *Rev. Mod. Phys.*, 83:943–999, Sep 2011.
- [27] Eric-Jan Wagenmakers and Simon Farrell. Aic model selection using akaike weights. *Psychonomic bulletin & review*, 11(1):192–196, 2004.
- [28] Steve Waterhouse, David MacKay, and Anthony Robinson. Bayesian methods for mixtures of experts. *Advances in neural information processing systems*, 8:351–357, 1995.
- [29] Max Welling and Yee W Teh. Bayesian learning via stochastic gradient langevin dynamics. In *Proceedings of the 28th international conference on machine learning (ICML-11)*, pages 681–688, 2011.
- [30] Kai Xu, Hong Ge, Will Tebbutt, Mohamed Tarek, Martin Trapp, and Zoubin Ghahramani. Advancedhmc.jl: A robust, modular and efficient implementation of advanced hmc algorithms. 2019.
- [31] Cagatay Yildiz, Markus Heinonen, and Harri Lahdesmaki. Ode2vae: Deep generative second order odes with bayesian neural networks. In *Advances in Neural Information Processing Systems*, pages 13412–13421, 2019.